Published in final edited form as:

Circulation. 2023 January 10; 147(2): 142–153. doi:10.1161/CIRCULATIONAHA.122.061130.

Cardiac Troponin I-interacting Kinase impacts cardiomyocyte S-phase activity but not cardiomyocyte proliferation

Sean P. Reuter, B.S.[1,2], **Mark H. Soonpaa, Ph.D.**[1,2], **Dorothy Field, M.S.**[1,2], **Ed Simpson, Ph.D.**[3], **Michael Rubart-von der Lohe, M.D.**[2], **Han Kyu Lee, Ph.D.**[5], **Arthi Sridhar, M.S.**[2], **Stephanie M. Ware, M.D./Ph.D.**[2], **Nick Green, B.S**[3], **Xiaochun Li, Ph.D.**[4], **Susan Ofner, M.S.**[4], **Douglas A. Marchuk, Ph.D.**[5], **Kai C. Wollert, M.D.**[6], **Loren J. Field, Ph.D.**[1,2,*]

[1]Krannert Cardiovascular Research Center, Indiana University School of Medicine

[2]Herman B Wells Center for Pediatric Research, Indiana University School of Medicine

[3]Center for Computational Biology & Bioinformatics, Indiana University School of Medicine

[4]Department of Biostatistics and Health Data Science, Indiana University School of Medicine

[5]Department of Molecular Genetics and Microbiology, Duke University School of Medicine

[6]Department of Cardiology and Angiology, Division of Molecular and Translational Cardiology, Hannover Medical School

Abstract

Background.—Identifying genetic variants which impact the level of cell cycle reentry and establishing the degree of cell cycle progression in those variants could help guide development of therapeutic interventions aimed at effecting cardiac regeneration. We observed that C57Bl6/NCR (B6N) mice have a marked increase in cardiomyocyte S-phase activity following permanent coronary artery ligation as compared to infarcted DBA/2J (D2J) mice.

Methods: Cardiomyocyte cell cycle activity post-infarction was monitored in D2J, (D2J × B6N)-F1 and [(D2J × B6N)-F1 × D2J] backcross mice via bromodeoxyuridine or 5-ethynyl-2'-deoxyuridine incorporation, using a nuclear-localized transgenic reporter to identify cardiomyocyte nuclei. Genome-wide quantitative trait locus (QTL) analysis, fine scale genetic mapping, whole exome sequencing and RNA-seq analyses of the backcross mice were performed to identify the gene responsible for the elevated cardiomyocyte S-phase phenotype.

Results: (D2J × B6N)-F1 mice exhibited a 14-fold increase in cardiomyocyte S-phase activity in ventricular regions remote from infarct scar as compared to D2J mice (0.798 ± 0.09% vs. 0.056 ± 0.004%; $p < 0.001$). QTL analysis of [(D2J × B6N)-F1 × D2J] backcross mice revealed that the

*Corresponding Author: Loren J. Field, Krannert Cardiovascular Research Center & Wells Center for Pediatric Research, 1044 West Walnut Street, Indianapolis, Indiana, USA 46202, 317 274 5085, ljfield@iu.edu.

Disclosures
None

Supplemental Materials:
Expanded Methods
Figures S1–S8
Table S1
Excel File S1

gene responsible for differential S-phase activity was located on the distal arm of Chromosome 3 (LOD score = 6.38; $p < 0.001$). Additional genetic and molecular analyses identified 3 potential candidates. Of these, troponin I-interacting kinase (*Tnni3k*) is expressed in B6N hearts but not in D2J hearts. Transgenic expression of Tnni3k in a D2J genetic background results in elevated cardiomyocyte S-phase activity post-injury. Cardiomyocyte S-phase activity in both TNNI3K-expressing and TNNI3K-nonexpressing mice results in the formation of polyploid nuclei.

Conclusions: These data indicate that TNNI3K expression increases the level of cardiomyocyte S-phase activity following injury.

Keywords

Cardiomyocyte cell cycle; heart regeneration

Introduction

Increases in cardiac mass during development result largely from the proliferation of contracting, albeit immature, cardiomyocytes.[1] During postnatal development, cardiomyocytes undergo a transition from hyperplastic to hypertrophic growth, which in rodents is accompanied by the formation of binucleated cells.[1–5] It is generally accepted that adult mammalian cardiomyocytes have only a very limited capacity for renewal, and that this renewal occurs via proliferation of preexisting cardiomyocytes as opposed to *de novo* cardiomyogenic differentiation of stem cells.[6] These low renewal rates, coupled with the much higher renewal rates observed for other cell types in the adult heart, make accurate quantitation of cardiomyocyte proliferation technically difficult.[7–9] Early studies using a 4 hour pulse of tritiated thymidine reported that, at any given time, only 0.0005% of the ventricular cardiomyocyte nuclei are in S-phase in uninjured adult DBA/2J (abbreviated D2J) mouse hearts.[10] Studies in humans exploiting the spike in atmospheric radioactive carbon resulting from numerous above-ground nuclear tests in the 1950s and 1960s, predicted an annual cardiomyocyte renewal rate of 1% per year in young humans.[11] Assuming a linear relationship, extrapolating the cardiomyocyte S-phase index during a 4 hour pulse of tritiated thymidine to a yearly incorporation rate gives a very similar value of cardiomyocytes undergoing S-phase per year in uninjured mouse hearts (i.e., 0.0005% × 24 hours/4 hour pulse × 365 or 1.09%). Myocardial injury is associated with a localized increase in cardiomyocyte S-phase activity, as evidenced by incorporation of modified nucleotides or expression of cell cycle markers.[1, 10, 12–14]

We have recently shown that treatment with the CXCR4 antagonist POL5551 resulted in enhanced angiogenesis in the infarct border zone, reduced scar size, and attenuated left ventricular remodeling and contractile dysfunction following ischemia/reperfusion injury.[15] In subsequent experiments testing the impact of POL5551 on cardiomyocyte proliferation in infarcted hearts, we unexpectedly observed that vehicle-treated mice in a C57Bl6/NCR (abbreviated B6N) genetic background have a much higher level of cardiomyocyte S-phase activity as compared to vehicle-treated mice in a D2J genetic background. Here, we show that the high levels of cardiomyocyte S-phase activity in infarcted B6N mice are due to the expression of TNNI3K. The results are discussed in the context of a recent study suggesting that loss of TNNI3K enhances myocardial regeneration in injured hearts.[16]

Methods

Please see Supplemental Materials section for an extended description of the methods used.

The authors declare that all supporting data are available within the article and its online supplementary files.

Mice.

Generation of the MHC-nLAC and TNNI3K^{tg} mice was described previously.[17, 18] Both lines were maintained in a D2J genetic background (Jackson Labs, Bar Harbor, Maine). C57Bl6/NCR mice were obtained from Charles River (St. Louis, Missouri). SWR/J (SWJ) and C57Bl6/J (B6J) mice were obtained from Jackson Labs. Animal husbandry and all experimental procedures were reviewed by the Indiana University Institutional Animal Care and Use Committee and performed in accordance with those guidelines.

Infarct Surgery.

Permanent coronary artery ligations were performed as described previously.[19] Osmotic mini-pumps (Alzet #2002; Cupertino, California) containing BrdU (16 mg/ml in phosphate buffered saline; Roche, Indianapolis, Indiana) or EdU (13.14 mg/ml in 10% DMSO) were implanted as described.[20]

Histology.

Tissues were harvested, fixed in cacodylic acid/ paraformaldehyde,[21] cryoprotected in 30% sucrose and sectioned at 10 microns using standard methodologies.[22] After antigen retrieval samples were processed for β-galactosidase (Invitrogen Life Technologies #A-11132; Grand Island, New York) and BrdU (Roche #11296736001; clone BMG 6H8 IgG1) using the Vector Mouse-on-Mouse kit (#BMK-2202, Burlingame, California). Signal was developed using Alexa 555-conjugated goat anti-rabbit and Alexa 488-conjugated goat anti-mouse secondary antibodies (Invitrogen Life Technologies #A21429 and #A11001, respectively). DNA was visualized with Hoechst 33342 (Invitrogen Life Technologies).

Quantitation of Cardiomyocyte S-phase Activity.

Sections were scanned sequentially for the red, green and blue color channels (βGAL immune reactivity, BrdU immune reactivity and Hoechst fluorescence, respectively) and image analyses performed as described in detail in the Extended Methods section. For each heart studied, a minimum of 5 four-chamber coronal sections traversing the infarct, sampled at a minimum of 100 micrometer intervals, were analyzed. For each section, the infarct, border zone, and remote ventricular myocardium were defined as described above. The cardiomyocyte labeling index is defined as the percentage of BrdU positive cardiomyocyte nuclei present in the analyzed region. For analyses of individual animals, the cardiomyocyte labeling index for a given anatomical region was determined for each section, and the mean value and SEM of each animal was calculated. For comparisons of different genotypes, the total cardiomyocyte labeling index for a given anatomical region in each individual mouse in a given genotype was determined, and then the average and SEM for the population was calculated.

Genotype analyses.

SNP genotype analyses were performed at the DartMouse™ Speed Congenic Core Facility at the Geisel School of Medicine, Dartmouth University. DartMouse uses the Illumina, Inc. (San Diego, CA) Infinium Genotyping Assay to interrogate a custom panel of 5307 SNPs. The raw SNP data were analyzed using DartMouse SNaP-Map™ and Map-Synth™ software. Restriction fragment length polymorphisms were used to identify crossover events in the distal arm of Chromosome 3.[23]

Quantitative Trait Locus (QTL) Analysis.

Genome-wide scans were performed using R/qtl software. Genotypes were prepared for QTL mapping; a total of 2,408 markers were chosen for mapping. The significance thresholds were determined by 1,000 permutations using all informative markers. A QTL was considered significant when its logarithm of the odds (LOD) score exceeded 95% ($p < 0.05$) of the permutation distribution. The 95% confidence interval (CI) of the peak was suggested by the R/qtl software (RStudio, version 1.3.1093). The physical map (megabase; Mb) positions based on the genome sequence from the GRCm38/mm10 were calculated using the Mouse Map Converter tool of the Jackson Laboratory (http://cgd.jax.org/mousemapconverter/).

WES and RNA-seq Analyses.

For WES, genomic DNA from D2J and B6N liver was isolated and used to generate libraries and sequenced, as described in the Extended Methods section. Variant annotation and analysis was done using SNP & Variation Suite v8.8.3 (Golden Helix, Inc., Bozeman, MT, www.goldenhelix.com).The potential impact of the sequence variants was interrogated using SIFT (Sorting Intolerant from Tolerant),[24] PROVEAN (Protein Variation Effect Analyzer),[25] SNAP2[26] and BLOSUM62[27]. For RNA-seq, total RNA was isolated and then used for cDNA library preparation and sequencing as described in the Extended Methods section. Differential gene expression was assessed using edgeR software[28] with a false discovery rate (FDR) threshold of 5%[29] and a low expression threshold of 1 cpm; a 25% change in expression was used as the cut-off for candidate gene selection.

Western Blot Analyses.

Hearts were homogenized and samples were resolved on SDS-PAGE gels30 electro-transferred to nitrocellulose membranes[31] as described in the Extended Methods section. Primary antibodies recognized mouse TNNI3K,[18] human TNNI3K,[32] and mouse anti-GAPDH (Novus Biologicals #NB300–221SS, Centennial, Colorado). Signal was visualized by the Amersham ECL method according to the manufacturer's protocol (Millipore Sigma).

Cardiomyocyte Nuclear Ploidy assay.

Hearts from MHC-nLAC mice labeled with EdU were subjected to retrograde collagenase perfusion as described[4] and the ventricles triturated in 2 ml of cacodylic acid/paraformaldehyde and filtered through a 100 micron strainer. After 20 minutes at room temperature, the cells were pelleted through several PBS washes and then smeared on Superfrost slides (Fischer Scientific, Hampton, New Hampshire) and dried overnight at

room temperature. Slides were stained with Click-iT® 488 (Invitrogen, Carlsbad, California) and incubated with Hoechst 33342, rinsed and cover slipped with Prolong Gold (Invitrogen). Putative EdU positive cardiomyocytes were identified and imaged on a Leica DM5500 microscope. The coverslips were then removed and the slides processed for βGAL immune reactivity as described above (the same fields were then imaged). The resulting image sets were analyzed using MetaMorph software. Nuclei (blue channel) were segmented using the Metamorph Count Nuclei application, and the Hoechst signal was quantitated to determine nuclear content. Cardiomyocyte nuclear identity and EdU positivity were confirmed by overlay of the red and green channels. The procedure is described in detail in the Extended Methods section.

Statistics.

A two independent sample *t*-test was used to compare cardiomyocyte S-phase activity between corresponding zones of D2J and (D2J × B6N)-F1 mice. *Kruskal-Wallis One Way Analysis of Variance on Ranks* was used for comparisons of cardiomyocyte S-phase labeling index for all pairwise combinations of any one zone in D2J hearts with any one zone in (D2J × B6N)-F1 hearts, and to compare cardiomyocyte S-phase activity in the remote myocardium of D2J, (D2J × B6N)-F1 and congenic mice heterozygous for the distal arm of chromosome 3 (the average of multiple sections per heart, and multiple hearts per genotype, were used). To estimate the predicted probability of cardiomyocyte nuclear content being in the non-cardiomyocyte (i.e., 2N control) group, a logistic model was used with independent terms of slide and DNA fluorescence. Statistics used for QTL, WES and RNA-seq analyses are described in those sections.

Results

D2J and B6N mice exhibit different patterns of cardiomyocyte S-phase activity following injury.

Transgenic mice which utilize the α-cardiac myosin heavy chain promoter to target cardiomyocyte-restricted expression of a nuclear-localized β-galactosidase reporter (MHC-nLAC mice) were developed previously to facilitate identification of cardiomyocyte nuclei in tissue sections.[17] We have used these mice to monitor the pattern of cardiomyocyte S-phase activity during the first two weeks post-infarction. Mice were subjected to permanent coronary artery ligation and implanted with an Alzet osmotic pump containing Bromodeoxyuridine (BrdU). The hearts were harvested 14 days later, sectioned, and processed for β-galactosidase (βGAL) and BrdU immune reactivity (Figure 1A, red and green signals, respectively). Cardiomyocyte nuclei with S-phase activity, as evidenced by the overlay of red and green signal in merged images of whole heart sections, were ringed to facilitate visualization of their anatomical position (Figure 1A, merged and ringed panels). Figure 1B shows the pattern of cumulative cardiomyocyte S-phase activity in an infarcted MHC-nLAC mouse maintained in an inbred D2J genetic background. The S-phase cardiomyocyte nuclei tended to reside in the endocardial layer and border zone (S-phase events were also detected in the infarct in other sections). At least a portion of the endocardial S-phase positive cells appear to be conduction system cardiomyocytes (Figure S1). Figure 1C shows the pattern of cumulative cardiomyocyte S-phase activity

in an infarcted MHC-nLAC mouse generated by backcrossing the reporter transgene into a B6N genetic background for 3 generations. Many S-phase cardiomyocyte nuclei in the B6N heart were apparent throughout the ventricular septum, the ventricular free walls and the papillary muscles (i.e., in regions remote from the infarct). Thus, the pattern of post-infarction cardiomyocyte S-phase activity differs markedly between D2J and B6N mice.

To quantitate this difference in cardiomyocyte S-phase activity, D2J and (D2J × B6N)-F1 mice were generated (all mice carried the MHC-nLAC reporter transgene). At 12 weeks of age the mice were subjected to permanent coronary artery ligation and implanted with BrdU osmotic pumps. Fourteen days later, the hearts were harvested and processed as described above. The cumulative 14-day cardiomyocyte labeling index (that is, the percentage of BrdU positive cardiomyocyte nuclei) was determined for the ventricular myocardium remote from the infarct, the infarct border zone and the infarct as shown (Figure 1D). Hearts from D2J mice exhibited low cumulative BrdU labeling indices in the ventricular myocardium remote from the infarct, averaging 0.056 ± 0.004% (n = 10 hearts). In contrast, the cumulative BrdU labeling index in the ventricular myocardium remote from the infarct from (D2J × B6N)-F1 hearts was higher, averaging 0.798 ± 0.09% (n = 17 hearts; $p < 0.001$ vs. the D2J group). The phenotypes were clearly separated, with no overlap in the cardiomyocyte labeling index values of individual animals in the D2J vs. the (D2J × B6N)-F1 genotypes (Figure 1E). Cardiomyocyte S-phase activity was also elevated in the infarct border zone of (D2J × B6N)-F1 mice as compared to D2J mice, but not in the infarct (Figure 1E). Interestingly, cardiomyocyte S-phase levels in uninjured hearts were also elevated in B6N vs. D2J mice (0.208 ± 0.045% vs. 0.028 ± 0.005%, $p<0.05$; n=8 B6N and 4 D2J hearts).

A gene contributing to elevated levels of cardiomyocyte S-phase activity post-injury resides on the distal arm of B6N chromosome 3.

To interrogate the genetic basis for this difference in cardiomyocyte S-phase activity, [(D2J × B6N)-F1 × D2J] backcross mice were generated (all mice carried the MHC-nLAC reporter transgene). At 12 weeks of age the mice were subjected to permanent coronary artery ligation, implanted with BrdU osmotic pumps and processed as described above. The cardiomyocyte labeling index was then determined for the ventricular regions remote from the infarct, as these regions exhibited the greatest difference in cardiomyocyte S-phase activity between the D2J and B6N backgrounds. Analysis of [(D2J × B6N)-F1 × D2J] backcross mice revealed that the cumulative cardiomyocyte labeling indices for individual animals fell into two distinct groups, with 17 animals having low labeling indices similar to those seen for D2J mice and 11 animals having comparatively higher labeling indices similar to those seen for (D2J × B6N)-F1 mice (Figure S2).

Genome-wide QTL linkage analysis was performed to map the genetic region(s) that regulate cardiomyocyte S-phase activity. The 28 animals generated from the [(D2J × B6N)-F1] × D2J backcross were genotyped using the Illumina Infinium Bead Chip and the data interrogated with Dart Mouse SNaP-Map Software. This analysis employed 2,408 informative single nucleotide polymorphism (SNP) markers (Excel File S1) that fully covered the mouse genome. A single QTL peak on chromosome 3 (LOD score, 6.38; p

< 0.001) that exhibits highly significant linkage to cardiomyocyte S-phase activity was identified (Figure 2).

To confirm that the gene(s) responsible for elevated levels of post-injury cardiomyocyte S-phase activity resides in this region, congenic mice which were heterozygous D2J/B6N for the distal arm of chromosome 3 (downstream of SNP rs6288253 at nucleotide 140,506,317), but which were otherwise homozygous D2J, were generated via sequential backcrossing into the D2J background (Figure 3A; these mice also carried the MHC-nLAC reporter). At 12 weeks of age, the mice were subjected to permanent coronary artery ligation, implanted with 14-day BrdU osmotic pumps, and processed as described above. Once again, S-phase cardiomyocyte nuclei were apparent throughout the entire ventricular myocardium (Figure 3B). The cumulative cardiomyocyte labeling index for ventricular regions remote from the infarct in the congenic mice was 0.656 ± 0.13% (n = 4 mice, $p < 0.05$ vs. the D2J group described above), confirming that the gene responsible for elevated cardiomyocyte S-phase activity resided on the distal arm of chromosome 3 as defined by the congenic mice. This 19.4 Mb interval carries 309 candidates (including coding, noncoding and unclassified genes).

Since the phenotype appears to be driven by a single, dominant locus, we performed fine-scale mapping as for a Mendelian trait, focusing on individual animals exhibiting a crossover within the interval. Multigenerational backcross animals were produced, and crossover events identified by the presence of heterozygosity for one or two restriction fragment length polymorphisms in the haplotype defined by SNPs rs3090379, rs13477506 and rs36403089 (located at nucleotides 142,041,673, 154,839,656 and159,812,056, respectively, see Figure S3). Mice exhibiting crossover events were subjected to permanent coronary artery ligation, BrdU labeling and then processed as described above (these mice also carried the MHC-nLAC reporter); mice exhibiting elevated levels of cardiomyocyte S-phase activity should share a common region of heterozygosity harboring the B6N allele responsible for the trait. Of 463 mice generated, 53 harbored crossover events within the interval; of these, 43 survived infarction of which 17 exhibited elevated levels of cardiomyocyte S-phase activity post-MI (defined as being ≥ 0.33%, the lowest S-phase labeling index observed for an individual infarcted (D2J × B6N)-F1 mouse, see Figure S2). Analysis of SNP distribution maps defined a region of interest (ROI) between nucleotides 151,564,321 and 156,149,851 which retained heterozygosity in all mice with elevated S-phase levels (Figure 4A; S-phase values for these animals are shown in Table S1). SNP analyses of whole exome sequencing (WES) datasets generated from mouse #65761 and #63328 further refined the positions of the crossover events in those animals, revealing that the gene responsible for elevated cardiomyocyte S-phase activity post-injury resides between nucleotides 153,678,445 and 156,149,851 on chromosome 3 (Figure 4B). This 2.5 Mb region carries 13 protein coding genes, 21 non-coding genes and 6 unclassified genes.

Tnni3k is responsible for elevated cardiomyocyte S-phase activity following myocardial injury.

WES (using DNA prepared from D2J and B6N mice to identify nucleotide variants) and RNA-Seq (using RNA prepared from infarcted D2J and B6N ventricle tissue remote from

the infarct to identify differentially expressed genes) analyses were employed to identify and stratify candidate genes within the ROI which might give rise to the phenotype. A total of 3 candidates were identified (*Tnni3k, Erich-3,* and *Fpgt*). WES revealed a previously identified A→G substitution in D2J mice at nucleotide 154,875,123 in the splice donor sequence in intron 19 on the coding strand of the *Tnni3k* gene. This substitution results in the incorporation of 4 additional nucleotides at the 3' end of exon 19, which gives rise to a frame shift and premature truncation of the protein in D2J mice and nonsense-mediated decay of the transcript, resulting in the lack of TNNI3K protein[18] (see also Figure S4). In addition, a C→T substitution was observed on the coding strand at nucleotide 154,709,772 in *Erich3* and a A→G substitution at nucleotide 155,086,840 in *Fpgt*, which resulted in nonsynonymous variants predicted by SNAP2[26] and BLOSUM62,[27] respectively, to be deleterious to protein function. RNA-Seq revealed a 3.57-fold decrease in expression of *Tnni3k* in D2J vs. B6N hearts (due at least in part to non-sense mediated decay of the aberrantly spliced transcript).[18]

Of these candidates, the *Tnni3k* gene has previously been implicated in cardiomyocyte cell cycle activity.[16] We have generated transgenic mice expressing a human *Tnni3k* cDNA under the regulation of the α-cardiac myosin heavy chain promoter.[18] These animals (maintained in an inbred D2J genetic background) were intercrossed with the MHC-nLAC reporter animals (also in a D2J genetic background); mice inheriting both the *Tnni3k* and MHC-nLAC transgenes (designated TNNI3K^{tg}) and mice inheriting only the MHC-nLAC reporter (designated Control) were identified and sequestered. At 12 weeks of age, the mice were subjected to permanent coronary artery ligation, BrdU infusion, and then the hearts were harvested and analyzed as described above. The Control mice exhibited low levels of cardiomyocyte S-phase activity, which was predominantly localized to the infarct and the infarct border zone (as was expected given that they are in a D2J genetic background, Figure 5A left panel). In contrast, cardiomyocyte S-phase activity in the TNNI3K^{tg} mice was apparent throughout the ventricle, and the level of S-phase activity was greater than that in the Control hearts (Figure 5A and B, respectively). Cardiomyocyte S-phase levels were not different between infarcted TNNI3K^{tg} and (D2J × B6N)-F1 mice (two-tailed P-value = 0.288). Western blot analyses with a human-specific TNNI3K antibody confirmed TNNI3K^{TG} transgene expression (Figure 5C).

The vast majority of cardiomyocyte S-phase events in the adult mouse heart result in increased nuclear ploidy, regardless of TNNI3K expression.

To determine if the presence or absence of TNNI3K expression impacts the ability of S-phase cardiomyocytes to progress through the cell cycle, D2J and B6N mice were subjected to permanent coronary artery ligation, followed by 2 weeks of infusion with the alkyne-containing nucleotide analogue 5-ethynyl-2'-deoxyuridine (EdU; all mice carried the MHC-nLAC reporter). The hearts were then harvested, and dispersed cell preparations were generated via collagenase digestion. The dispersed cells were affixed to microscope slides and processed with azide-containing Alexa 488 Click-iT reagent (which forms a covalent bond with EdU; green signal) to identify S-phase positive cardiomyocytes, and with Hoechst (blue signal) to visualize DNA content (Figure 6A, upper panels). Fields with S-phase positive cardiomyocytes were imaged in the blue channel at 2-micron intervals

in the *z*-axis such that entire nuclei were captured, and total Hoechst signal per nucleus quantitated. Finally, the identities of the cardiomyocyte nuclei were confirmed based on βGAL immune reactivity (Figure 6A, lower panels). In addition to the EdU-positive cardiomyocytes, DNA content was scored in EdU-negative non-cardiomyocyte nuclei, EdU-negative mononucleated cardiomyocyte nuclei and EdU-negative binucleated cardiomyocyte nuclei which were present in the same field. DNA content was normalized to that in the EdU-negative non-cardiomyocyte population, which was presumed to have a predominately diploid (2N) DNA content.

In D2J (TNNI3K-negative) hearts, the median DNA content of EdU-positive nuclei in mononucleated and binucleated cardiomyocytes was 2.19- and 2.00-fold, respectively, of that observed in the EdU-negative noncardiomyocyte population, with very little overlap in the DNA content between individual nuclei in the cardiomyocyte vs. noncardiomyocyte groups (Figure 6B). This indicates that the vast majority of S-phase events in D2J cardiomyocytes results in the formation of polyploid nuclei. EdU-positive cardiomyocyte nuclei remained polyploid after a 2-day chase period (accomplished by surgical removal of the EdU osmotic pump, Figure S5). In contrast, DNA content in the majority of EdU-negative cardiomyocyte nuclei was similar to that seen in the non-myocyte population, indicating that they were 2N. In B6N (TNNI3K-positive) hearts, the median DNA content of the EdU-positive nuclei in mononucleated and binucleated cardiomyocytes was 2.64- and 1.81-fold, respectively, of that observed in the EdU-negative noncardiomyocyte population, with very little overlap in DNA content between the cardiomyocyte and noncardiomyocyte groups (Figure 6C). These data are again consistent with cardiomyocyte S-phase events giving rise to polyploid nuclei. Overall, using a predicted probability of > 20% as the threshold for a given cardiomyocyte nucleus having a 2N DNA content, 99.5% and 96.6% of the EdU-positive cardiomyocyte nuclei from D2J and B6N hearts, respectively, were polyploid (Figure S6). Interestingly, the increased S-phase activity in B6N hearts preferentially impacted the binucleated cardiomyocyte population. In support of the absence of further cell cycle progression, only one cardiomyocyte nucleus with phosphohistone-H3 immune reactivity was observed when screening 130,996 cardiomyocyte nuclei distributed amongst 5 infarcted B6N hearts (0.00076%, see also Figure S7).

Discussion

This study sought to identify the genetic basis for the surprising 14-fold increase in cardiomyocyte S-phase activity observed in the remote myocardium following permanent coronary artery ligation in (D2J × B6N)-F1 versus D2J mice. Genome-wide QTL mapping, congenic mouse analyses, and fine scale mapping studies indicated that the responsible gene resided in a 2.5 Mb region of the B6N chromosome 3, while WES and RNA-seq analyses identified 3 candidates. One candidate gene, *Tnni3k*, was expressed in B6N hearts but not in D2J hearts, and transgenic expression of human TNNI3K in a D2J genetic background resulted in increased cardiomyocyte S-phase activity post-MI which was not different from that in (D2J × B6N)-F1 animals. Collectively, these data indicate that the differential levels of cardiomyocyte S-phase activity post-MI in B6N vs. D2J mice is due to differential expression of TNNI3K.

The biological function of TNNI3K is not fully understood. The gene encodes a cardiac-specific kinase with sequence homology and domain structure similar to Integrin-Linked Kinase. The target(s) of its kinase activity remain largely unknown, with the exception of troponin I.[33] *In vivo*, TNNI3K protein is located at the cardiac sarcomeric Z-disc[32] where it modulates contractile function.[32, 33] Interestingly, multiple QTL mapping studies for different cardiac traits have identified this locus, and ultimately, this gene, to be responsible for the observed phenotypic variation observed across inbred strains of mice.[16, 18, 34–36] This convergence of seemingly distinct cardiac phenotypes on this single gene is likely due to three factors. First, the SNP giving rise to aberrant Tnni3k splicing (rs49812611) is effectively a null allele, as opposed to most common SNPs which very rarely result in complete loss of activity. Second, this Tnni3k null allele is fixed in approximately 50% of the commonly used inbred strains. Third, TNNI3K encodes a kinase which is located at sarcomeric Z disk and is known to interact with proteins regulating cardiac contractile activity. Thus, many crosses between any two randomly chosen inbred mouse strains will likely be segregating a null allele of a critically important protein for cardiomyocyte and heart function.

It is also well established that myocardial injury results in localized increases in cardiomyocyte S-phase activity.[1, 10, 12–14] In agreement with this, BrdU-positive cardiomyocyte nuclei in D2J mice lacking TNNI3K expression were readily detected in the infarct scar, and dropped precipitously in regions remote from the site of injury. Given the nature of the permanent coronary artery occlusion model, the cardiomyocytes which survive in the border zone and the infarct are subjected to chronic ischemia and concomitant oxidative stress.[37, 38] It is interesting to note that TNNI3K expression has been shown to increase oxidative stress throughout the myocardium following regional ischemic injury.[39] In this regard it is striking that TNNI3K expression also resulted in a propensity for cardiomyocyte S-phase activity in the remote myocardium similar to that seen for cardiomyocytes in the scar of mice lacking TNNI3K (Figure 1E). The higher levels of oxidative stress in the remote myocardium of infarcted TNNI3K-expressing hearts may contribute to the observed elevated levels of cardiomyocyte S-phase activity simply by making the myocardium more permissive for cell cycle reentry. This notion is supported by the increased S-phase levels seen in uninjured B6N vs. D2J hearts. The similarly elevated S-phase levels observed within the infarct zone (the region with greatest oxidative stress) of D2J vs. B6N hearts (Figure 1E) suggests that the maximal capacity of cardiomyocyte cell cycle reentry may not differ greatly in D2J vs. B6N mice. Although KEGG analysis of differentially expressed genes in infarcted B6N vs. D2J hearts suggests several candidate pathways (Figure S8), the underlying mechanism by which TNNI3K expression facilitates cardiomyocyte cell cycle reentry remains unclear.

Analysis of dispersed cell preparations indicated that the vast majority of cardiomyocyte S-phase events following myocardial infarction resulted in the formation of polyploid nuclei. The observation that S-phase activity resulted in polyploid nuclei in both mononucleated and binucleated cardiomyocytes is in agreement with a recent study showing that these two cell types are transcriptionally homogenous.[40] These data also indicated that the presence or absence of TNNI3K protein did not appreciably impact the ability of cardiomyocytes with S-phase activity to further progress through the cell cycle over the time-course studied. The

rare EdU-positive 2N nuclei observed in our analyses resided in binucleated cardiomyocytes. The assay used cannot determine if those rare cells were derived from a mononucleated 2N cardiomyocyte which progressed through S-phase and then karyokinesis (but not cytokinesis), or alternatively from a binucleated 2N, 2N cardiomyocyte which progressed through S-phase, karyokinesis and cytokinesis. It is however clear that the vast majority of cardiomyocytes entering the cell cycle in the adult mouse heart do not progress past S-phase. In contrast, if each cardiomyocyte exhibiting S-phase activity in TNNI3K-expressing mice had the ability to progress through cytokinesis, a 50% loss of cardiomyocytes (as was encountered in the infarct border zone in the current study) would be replaced over the course of 569 days (calculated simply by applying the Compound Interest Law).[41]

A previous study has implicated TNNI3K in myocardial regeneration. That study[16] reported that strains harboring the splice donor mutation in the *Tnni3k* gene (and thus lacking TNNI3K expression) exhibited an increase in the 2N mononuclear cardiomyocyte content in adult hearts as compared to strains expressing TNNI3K. Additional analyses of a small subset of these strains suggested that the absence of TNNI3K protein expression results in a 3-fold increase in cardiomyocyte S-phase activity in the infarct border zone following permanent coronary artery ligation. Analysis of dispersed cell preparations from hearts of infarcted EdU-labeled mice lacking TNNI3K expression revealed that approximately 80% of the label was incorporated into mononuclear cardiomyocytes, while analysis of isolated nuclei preparations revealed that approximately 80% of the label resided in 2N cardiomyocyte nuclei. These observations led the authors to conclude that roughly two thirds of the mononuclear cardiomyocytes entering S-phase in mice lacking TNNI3K expression progressed through cytokinesis. Similar results were observed following conditional or global Cre recombinase-mediated deletion of *Tnni3k* in C57Bl6/J mice harboring floxed alleles.[16]

In agreement with this early study, we observed a propensity for a higher (albeit variable, see Figure 6 vs. Figure S5) 2N mononuclear cardiomyocyte content in mice lacking TNNI3K expression (D2J) as compared to those expressing TNNI3K (B6N), however the pattern and magnitude of cardiomyocyte cell cycle activity following permanent coronary artery ligation were dramatically different. Specifically, the level of cardiomyocyte S-phase activity was much higher and the anatomic distribution of S-phase activity was greater in mice with TNNI3K expression as compared to mice lacking TNNI3K expression, the opposite of what was reported previously. In addition, the vast majority of cardiomyocyte S-phase events resulted in the formation of polyploid nuclei, irrespective of the presence or absence of TNNI3K protein expression.

The basis for the differential results is not obvious. Both studies utilized the same injury model, utilized incorporation of modified nucleotides to quantitate S-phase activity, quantitated DNA content to determine ploidy, and convincingly documented the presence or absence of TNNI3K expression in the different models employed. Moreover, preliminary analysis of Tnni3k-deficient [(SWJ × B6N)-F1) × SWJ] backcross mice did not detect EdU-positive 2N mononuclear cardiomyocytes (Soonpaa, unpublished observation); SWJ mice were previously reported to exhibit regenerative activity which was attributed to the lack of TNNI3K.[16] This suggests that the absence of overt cell cycle progression in EdU-positive

mononuclear cardiomyocytes in the D2J mice is not simply due to the presence a dominant inhibitory gene in that background. One technical difference is that the current study utilized a cardiomyocyte-restricted reporter to aid in the identification of cardiomyocyte nuclei for all cell cycle and ploidy analyses; this reporter has been used extensively in the past to quantitate cardiomyocyte S-phase activity.[3, 10, 21, 42–50] The penetrance of transgene expression in the MHC-nLAC mice is very high,[17, 46] precluding the possibility of missing events in TNNI3K-defficent mice of the magnitude reported previously.[16]

In summary, the data presented here indicate that mice expressing TNNI3K have markedly elevated levels of cardiomyocyte S-phase activity following permanent coronary artery ligation, as compared to mice lacking TNNI3K. This surprising level of intrinsic cardiomyocyte cell cycle reentry would lead to significant regenerative growth if each cardiomyocyte exhibiting S-phase activity was able to progress through cytokinesis. This in turn suggests that identification of factors which facilitate cardiomyocyte cell cycle progression beyond S-phase will be key to unlocking the intrinsic regenerative capacity of the heart.

Supplementary Material

Refer to Web version on PubMed Central for supplementary material.

Source of Funding

This work was support by National Institute of Health grants HL132927 & HL155218 (LJF), HL134599 (SMW) and HL083155 (DAM).

Non-standard Abbreviations and Acronyms

B6N	C57Bl6/NCR
D2J	DBA/2J
QTL	quantitative trait locus
Tnni3k	troponin I-interacting kinase
SWR	SWR/J
B6J	C57Bl6/J
βGAL	beta-galactosidase
WES	whole exome sequencing
SNP	single nucleotide polymorphism
BrdU	bromodeoxyuridine
ROI	region of interest
LOD	logarithm of the odds

Mb	megabase
EdU	5-ethyl-2'-deoxyuridine
KEGG	Kyoto encyclopedia of genes and genomes

References

1. Rumyantsev PP. Growth and hyperplasia of cardiac muscle cells. London, U.K.; New York, N.Y., U.S.A.: Harwood Academic Publishers; 1991.
2. Li F, Wang X, Capasso JM and Gerdes AM. Rapid transition of cardiac myocytes from hyperplasia to hypertrophy during postnatal development. J Mol Cell Cardiol. 1996;28:1737–46. [PubMed: 8877783]
3. Soonpaa MH, Zebrowski DC, Platt C, Rosenzweig A, Engel FB and Field LJ. Cardiomyocyte cell-cycle activity during preadolescence. Cell. 2015;163:781–2. [PubMed: 26544927]
4. Soonpaa MH, Kim KK, Pajak L, Franklin M and Field LJ. Cardiomyocyte DNA synthesis and binucleation during murine development. Am J Physiol. 1996;271:H2183–9. [PubMed: 8945939]
5. Alkass K, Panula J, Westman M, Wu TD, Guerquin-Kern JL and Bergmann O. No evidence for cardiomyocyte number expansion in preadolescent mice. Cell. 2015;163:1026–36. [PubMed: 26544945]
6. Eschenhagen T, Bolli R, Braun T, Field LJ, Fleischmann BK, Frisen J, Giacca M, Hare JM, Houser S, Lee RT, Marban E, Martin JF, Molkentin JD, Murry CE, Riley PR, Ruiz-Lozano P, Sadek HA, Sussman MA and Hill JA. Cardiomyocyte regeneration: a consensus statement. Circulation. 2017;136:680–686. [PubMed: 28684531]
7. Soonpaa MH, Rubart M and Field LJ. Challenges measuring cardiomyocyte renewal. Biochim Biophys Acta. 2013;1833:799–803. [PubMed: 23142641]
8. Soonpaa MH and Field LJ. Survey of studies examining mammalian cardiomyocyte DNA synthesis. Circ Res. 1998;83:15–26. [PubMed: 9670914]
9. Ang KL, Shenje LT, Reuter S, Soonpaa MH, Rubart M, Field LJ and Galinanes M. Limitations of conventional approaches to identify myocyte nuclei in histologic sections of the heart. Am J Physiol Cell Physiol. 2010;298:C1603–9. [PubMed: 20457832]
10. Soonpaa MH and Field LJ. Assessment of cardiomyocyte DNA synthesis in normal and injured adult mouse hearts. Am J Physiol. 1997;272:H220–6. [PubMed: 9038941]
11. Bergmann O, Bhardwaj RD, Bernard S, Zdunek S, Barnabe-Heider F, Walsh S, Zupicich J, Alkass K, Buchholz BA, Druid H, Jovinge S and Frisen J. Evidence for cardiomyocyte renewal in humans. Science. 2009;324:98–102. [PubMed: 19342590]
12. Hesse M, Bednarz R, Carls E, Becker C, Bondareva O, Lother A, Geisen C, Dressen M, Krane M, Roell W, Hein L, Fleischmann BK and Gilsbach R. Proximity to injury, but neither number of nuclei nor ploidy define pathological adaptation and plasticity in cardiomyocytes. J Mol Cell Cardiol. 2021;152:95–104. [PubMed: 33290769]
13. Meckert PC, Rivello HG, Vigliano C, Gonzalez P, Favaloro R and Laguens R. Endomitosis and polyploidization of myocardial cells in the periphery of human acute myocardial infarction. Cardiovasc Res. 2005;67:116–23. [PubMed: 15949475]
14. van Amerongen MJ, Harmsen MC, Petersen AH, Popa ER and van Luyn MJ. Cryoinjury: a model of myocardial regeneration. Cardiovasc Pathol. 2008;17:23–31. [PubMed: 18160057]
15. Wang Y, Dembowsky K, Chevalier E, Stuve P, Korf-Klingebiel M, Lochner M, Napp LC, Frank H, Brinkmann E, Kanwischer A, Bauersachs J, Gyongyosi M, Sparwasser T and Wollert KC. C-X-C Motif Chemokine Receptor 4 Blockade Promotes Tissue Repair After Myocardial Infarction by Enhancing Regulatory T Cell Mobilization and Immune-Regulatory Function. Circulation. 2019;139:1798–1812. [PubMed: 30696265]
16. Patterson M, Barske L, Van Handel B, Rau CD, Gan P, Sharma A, Parikh S, Denholtz M, Huang Y, Yamaguchi Y, Shen H, Allayee H, Crump JG, Force TI, Lien CL, Makita T, Lusis AJ, Kumar SR and Sucov HM. Frequency of mononuclear diploid cardiomyocytes underlies natural variation in heart regeneration. Nat Genet. 2017;49:1346–1353. [PubMed: 28783163]

17. Soonpaa MH, Koh GY, Klug MG and Field LJ. Formation of nascent intercalated disks between grafted fetal cardiomyocytes and host myocardium. Science. 1994;264:98–101. [PubMed: 8140423]
18. Wheeler FC, Tang H, Marks OA, Hadnott TN, Chu PL, Mao L, Rockman HA and Marchuk DA. Tnni3k modifies disease progression in murine models of cardiomyopathy. PLoS genetics. 2009;5:e1000647. [PubMed: 19763165]
19. Murry CE, Soonpaa MH, Reinecke H, Nakajima H, Nakajima HO, Rubart M, Pasumarthi KB, Virag JI, Bartelmez SH, Poppa V, Bradford G, Dowell JD, Williams DA and Field LJ. Haematopoietic stem cells do not transdifferentiate into cardiac myocytes in myocardial infarcts. Nature. 2004;428:664–8. [PubMed: 15034593]
20. Soonpaa MH and Field LJ. Assessment of cardiomyocyte DNA synthesis during hypertrophy in adult mice. Am J Physiol. 1994;266:H1439–45. [PubMed: 8184922]
21. Soonpaa MH, Koh GY, Pajak L, Jing S, Wang H, Franklin MT, Kim KK and Field LJ. Cyclin D1 overexpression promotes cardiomyocyte DNA synthesis and multinucleation in transgenic mice. J Clin Invest. 1997;99:2644–54. [PubMed: 9169494]
22. Junqueira LCU, Carneiro J and Kelley RO. Basic histology. 7th ed. Norwalk, Conn.: Appleton & Lange; 1992.
23. Sambrook J, Fritsch EF and Maniatis T. Molecular cloning : a laboratory manual. 2nd ed. Cold Spring Harbor, N.Y.: Cold Spring Harbor Laboratory; 1989.
24. Sim NL, Kumar P, Hu J, Henikoff S, Schneider G and Ng PC. SIFT web server: predicting effects of amino acid substitutions on proteins. Nucleic Acids Res. 2012;40:W452–7. [PubMed: 22689647]
25. Choi Y and Chan AP. PROVEAN web server: a tool to predict the functional effect of amino acid substitutions and indels. Bioinformatics (Oxford, England). 2015;31:2745–7. [PubMed: 25851949]
26. Hecht M, Bromberg Y and Rost B. Better prediction of functional effects for sequence variants. BMC Genomics. 2015;16 Suppl 8:S1.
27. Henikoff S and Henikoff JG. Amino acid substitution matrices from protein blocks. Proc Natl Acad Sci U S A. 1992;89:10915–9. [PubMed: 1438297]
28. Robinson MD, McCarthy DJ and Smyth GK. edgeR: a bioconductor package for differential expression analysis of digital gene expression data. Bioinformatics (Oxford, England). 2010;26:139–40. [PubMed: 19910308]
29. Aubert J, Bar-Hen A, Daudin JJ and Robin S. Determination of the differentially expressed genes in microarray experiments using local FDR. BMC Bioinformatics. 2004;5:125. [PubMed: 15350197]
30. Laemmli UK. Cleavage of structural proteins during the assembly of the head of bacteriophage T4. Nature. 1970;227:680–5. [PubMed: 5432063]
31. Towbin H, Staehelin T and Gordon J. Electrophoretic transfer of proteins from polyacrylamide gels to nitrocellulose sheets: procedure and some applications. Proc Natl Acad Sci U S A. 1979;76:4350–4. [PubMed: 388439]
32. Tang H, Xiao K, Mao L, Rockman HA and Marchuk DA. Overexpression of TNNI3K, a cardiac-specific MAPKKK, promotes cardiac dysfunction. J Mol Cell Cardiol. 2013;54:101–11. [PubMed: 23085512]
33. Wang H, Wang L, Song L, Zhang YW, Ye J, Xu RX, Shi N and Meng XM. TNNI3K is a novel mediator of myofilament function and phosphorylates cardiac troponin I. Brazilian journal of medical and biological research = Revista brasileira de pesquisas medicas e biologicas / Sociedade Brasileira de Biofisica [et al]. 2013;46:128–37.
34. Wiltshire SA, Leiva-Torres GA and Vidal SM. Quantitative trait locus analysis, pathway analysis, and consomic mapping show genetic variants of Tnni3k, Fpgt, or H28 control susceptibility to viral myocarditis. Journal of immunology. 2011;186:6398–405.
35. Lodder EM, Scicluna BP, Milano A, Sun AY, Tang H, Remme CA, Moerland PD, Tanck MW, Pitt GS, Marchuk DA and Bezzina CR. Dissection of a quantitative trait locus for PR interval duration identifies Tnni3k as a novel modulator of cardiac conduction. PLoS genetics. 2012;8:e1003113. [PubMed: 23236294]

36. Gan P, Patterson M, Velasquez A, Wang K, Tian D, Windle JJ, Tao G, Judge DP, Makita T, Park TJ and Sucov HM. Tnni3k alleles influence ventricular mononuclear diploid cardiomyocyte frequency. PLoS genetics. 2019;15:e1008354. [PubMed: 31589606]
37. Lindsey ML, Bolli R, Canty JM Jr., Du XJ, Frangogiannis NG, Frantz S, Gourdie RG, Holmes JW, Jones SP, Kloner RA, Lefer DJ, Liao R, Murphy E, Ping P, Przyklenk K, Recchia FA, Schwartz Longacre L, Ripplinger CM, Van Eyk JE and Heusch G. Guidelines for experimental models of myocardial ischemia and infarction. Am J Physiol Heart Circ Physiol. 2018;314:H812–H838. [PubMed: 29351451]
38. Kobayashi K, Maeda K, Takefuji M, Kikuchi R, Morishita Y, Hirashima M and Murohara T. Dynamics of angiogenesis in ischemic areas of the infarcted heart. Sci Rep. 2017;7:7156. [PubMed: 28769049]
39. Vagnozzi RJ, Gatto GJ Jr., Kallander LS, Hoffman NE, Mallilankaraman K, Ballard VL, Lawhorn BG, Stoy P, Philp J, Graves AP, Naito Y, Lepore JJ, Gao E, Madesh M and Force T. Inhibition of the cardiomyocyte-specific kinase TNNI3K limits oxidative stress, injury, and adverse remodeling in the ischemic heart. Sci Transl Med. 2013;5:207ra141.
40. Yekelchyk M, Guenther S, Preussner J and Braun T. Mono- and multi-nucleated ventricular cardiomyocytes constitute a transcriptionally homogenous cell population. Basic Res Cardiol. 2019;114:36. [PubMed: 31399804]
41. Blackman VH. The Compound Interest Law and Plant Growth. Annals of Botany. 1919;os-33:353–360.
42. Zhu W, Reuter S and Field LJ. Targeted expression of cyclin D2 ameliorates late stage anthracycline cardiotoxicity. Cardiovasc Res. 2019;115:960–965. [PubMed: 30423020]
43. Zaruba MM, Zhu W, Soonpaa MH, Reuter S, Franz WM and Field LJ. Granulocyte colony-stimulating factor treatment plus dipeptidylpeptidase-IV inhibition augments myocardial regeneration in mice expressing cyclin D2 in adult cardiomyocytes. Eur Heart J. 2012;33:129–37. [PubMed: 21849352]
44. Toischer K, Zhu W, Hunlich M, Mohamed BA, Khadjeh S, Reuter SP, Schafer K, Ramanujam D, Engelhardt S, Field LJ and Hasenfuss G. Cardiomyocyte proliferation prevents failure in pressure overload but not volume overload. J Clin Invest. 2017;127:4285–4296. [PubMed: 29083322]
45. Toischer K, Rokita AG, Unsold B, Zhu W, Kararigas G, Sossalla S, Reuter SP, Becker A, Teucher N, Seidler T, Grebe C, Preuss L, Gupta SN, Schmidt K, Lehnart SE, Kruger M, Linke WA, Backs J, Regitz-Zagrosek V, Schafer K, Field LJ, Maier LS and Hasenfuss G. Differential cardiac remodeling in preload versus afterload. Circulation. 2010;122:993–1003. [PubMed: 20733099]
46. Reuter S, Soonpaa MH, Firulli AB, Chang AN and Field LJ. Recombinant neuregulin 1 does not activate cardiomyocyte DNA synthesis in normal or infarcted adult mice. PLoS ONE. 2014;9:e115871. [PubMed: 25545368]
47. Pasumarthi KB, Nakajima H, Nakajima HO, Soonpaa MH and Field LJ. Targeted expression of cyclin D2 results in cardiomyocyte DNA synthesis and infarct regression in transgenic mice. Circ Res. 2005;96:110–8. [PubMed: 15576649]
48. Pasumarthi KB, Nakajima H, Nakajima HO, Jing S and Field LJ. Enhanced cardiomyocyte DNA synthesis during myocardial hypertrophy in mice expressing a modified TSC2 transgene. Circ Res. 2000;86:1069–77. [PubMed: 10827137]
49. Nakajima H, Nakajima HO, Tsai SC and Field LJ. Expression of mutant p193 and p53 permits cardiomyocyte cell cycle reentry after myocardial infarction in transgenic mice. Circ Res. 2004;94:1606–14. [PubMed: 15142950]
50. Nakajima H, Nakajima HO, Dembowsky K, Pasumarthi KB and Field LJ. Cardiomyocyte cell cycle activation ameliorates fibrosis in the atrium. Circ Res. 2006;98:141–8. [PubMed: 16306446]

Clinical Perspective

What is new?

- The study shows that mice which express Cardiac Troponin I-interacting Kinase (TNNI3K) exhibit higher levels of cardiomyocyte S-phase activity following injury as opposed to mice which do not express TNNI3K.
- The vast majority of cardiomyocytes S-phase events results in the formation of polyploid nuclei without further cell cycle progression, and further cell cycle progression is not influenced by the presence or absence of TNNI3K expression.

What are the clinical implications?

- The level of cardiomyocyte cell cycle reentry in hearts expressing TNNI3K would lead to significant regenerative growth if each cardiomyocyte exhibiting S-phase activity was able to progress through cytokinesis.
- This in turn suggests that identification of factors which facilitate cardiomyocyte cell cycle progression beyond S-phase will be key to unlocking the intrinsic regenerative capacity of the heart.

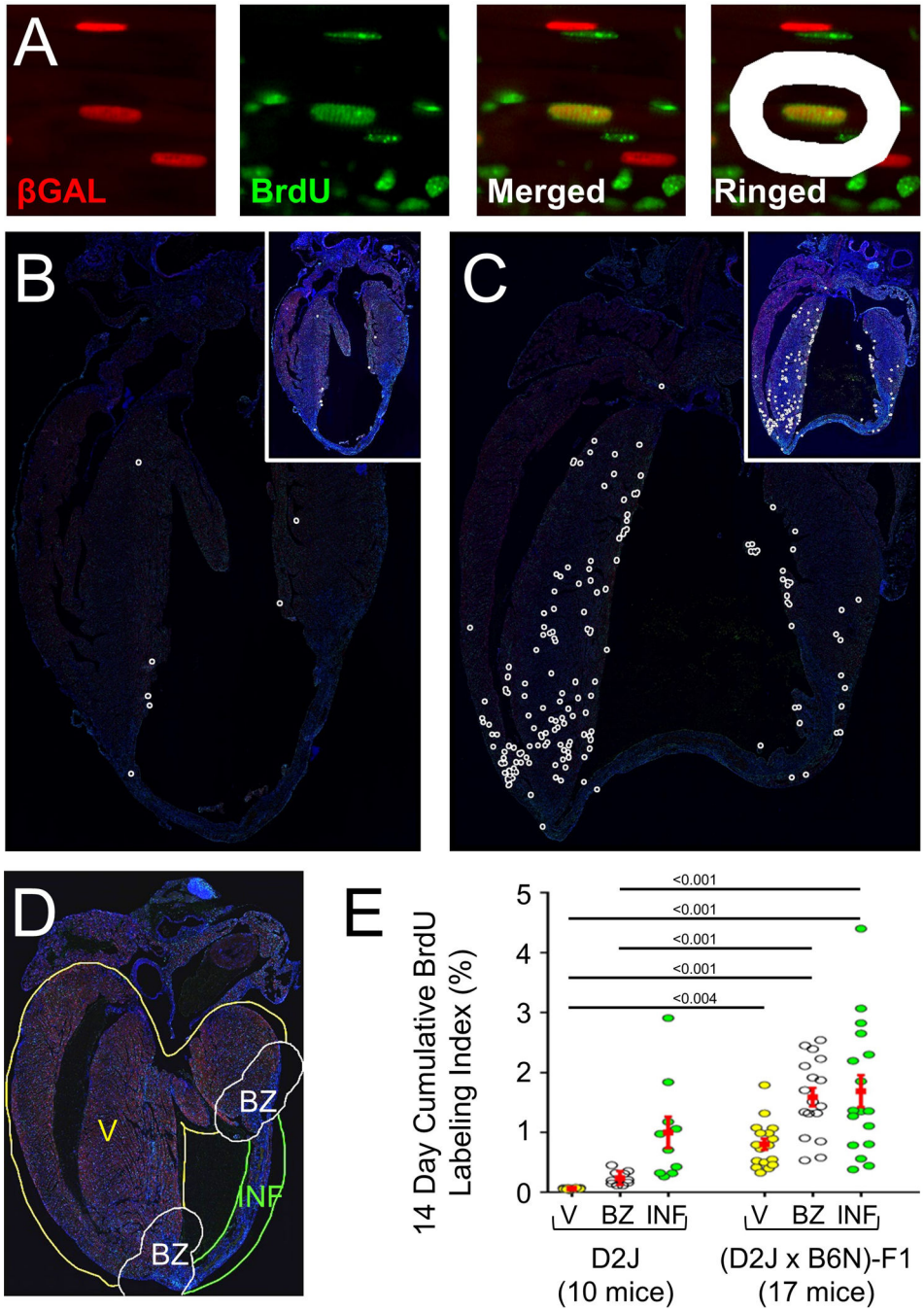

Figure 1.

Pattern of cardiomyocyte DNA synthesis in D2J and B6N genetic backgrounds following infarction. (A) Example of an S-phase cardiomyocyte using the MHC-nLAC reporter. The first panel shows βGAL immune reactivity (red secondary antibody), the second panel shows BrdU immune reactivity (green secondary antibody), the third panel shows a merged image (yellow indicates co-localization of βGAL and BrdU immune reactivity, and the fourth panel shows the computer-generated ring to mark the anatomical position of the S-phase event. (B) Representative example of the pattern of cardiomyocyte S-phase activity

in the heart from an infarcted D2J mouse. White rings indicate the anatomical positions of the S-phase cardiomyocyte nuclei; inset shows the same image with the brightness adjusted to facilitate visualization of the infarct anatomy at low magnification. (C) Representative example of the pattern of cardiomyocyte S-phase activity in the heart from an infarcted third-generation B6N backcross mouse. White rings indicate the anatomical positions of the S-phase cardiomyocyte nuclei; inset shows the same image with the brightness adjusted to facilitate visualization of the infarct anatomy at low magnification. (D) Computer-assisted parsing of an image of a heart into the ventricle remote from the infarct, the infarct border zone and the infarct (defined by the yellow, white and green traces, respectively). (E) Comparison of the cumulative cardiomyocyte S-phase labeling index in the remote ventricle (V), infarct border zone (BZ) and infarct (INF) myocardium after 14 days BrdU infusion post-injury. Yellow, white, and green dots indicate the V, BZ and INF labeling indices, respectively, per each one of 10 DJ2 mice and 17 (D2J × B6N)-F1 mice. Red symbols and vertical red lines indicate the mean labeling index and SEM, respectively, for each genotype. Kruskal – Wallis One Way Analysis on Ranks and Dunn’s method for Multiple Comparisons were used to compare labeling indices of each zone in D2J with each zone in (D2Jx B6N)-F1. p values for statistically significant differences are indicated.

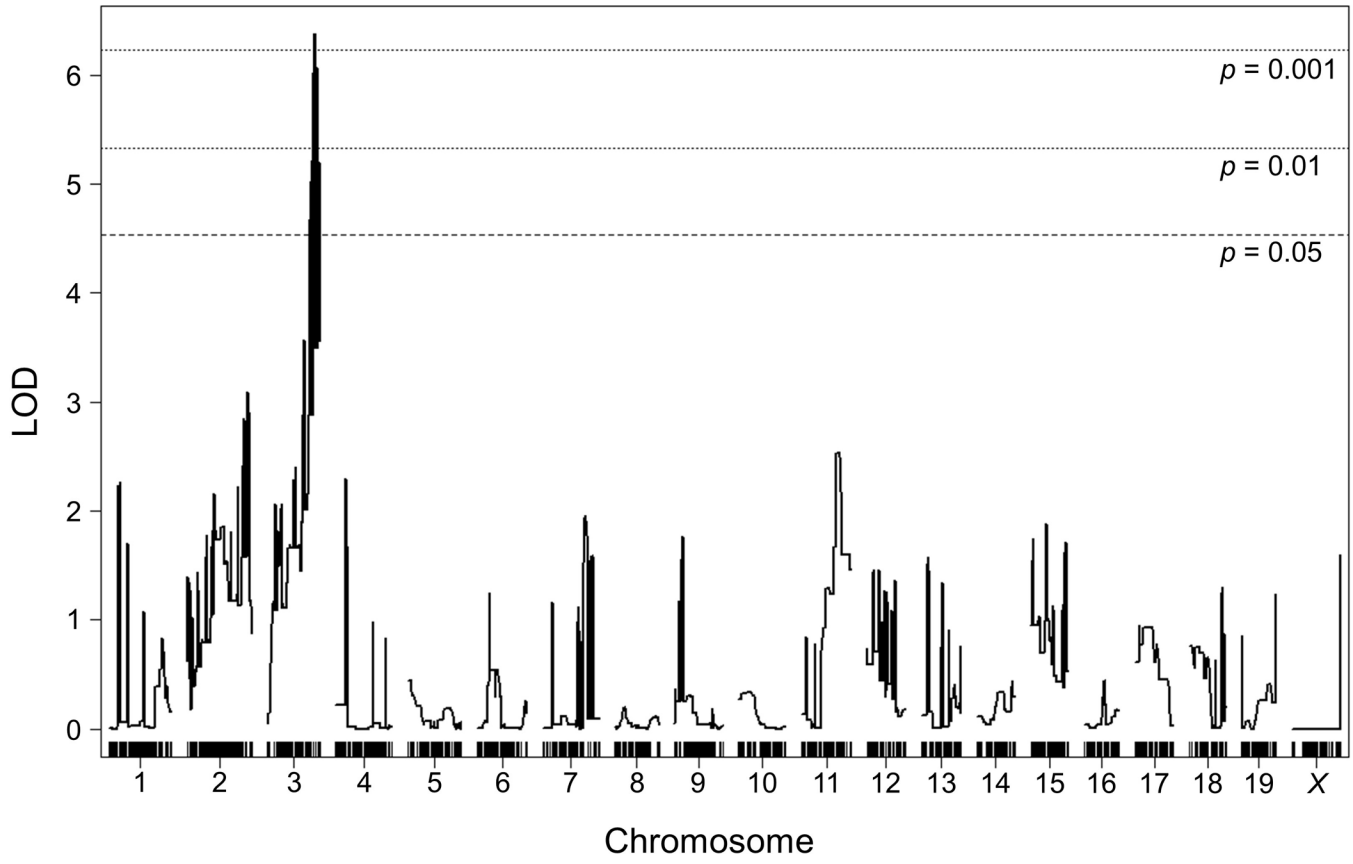

Figure 2.

Mapping a locus which contributes to high levels of cardiomyocyte S-phase activity following infarction. The graph shows a genome-wide QTL linkage scan for cardiomyocyte S-phase activity using 28 animals from a [(D2J × B6N)-F1] × D2J backcross. Chromosomes 1 through X are indicated numerically on the *x*-axis. The *y*-axis shows the logarithm of the odds (LOD) score. Levels of significance ($p < 0.05$, 0.01, and 0.001) were determined by a permutation test; 1,000 permutations of the data. A single genomic region on chromosome 3 displays a highly significant linkage peak, with a LOD score of 6.38.

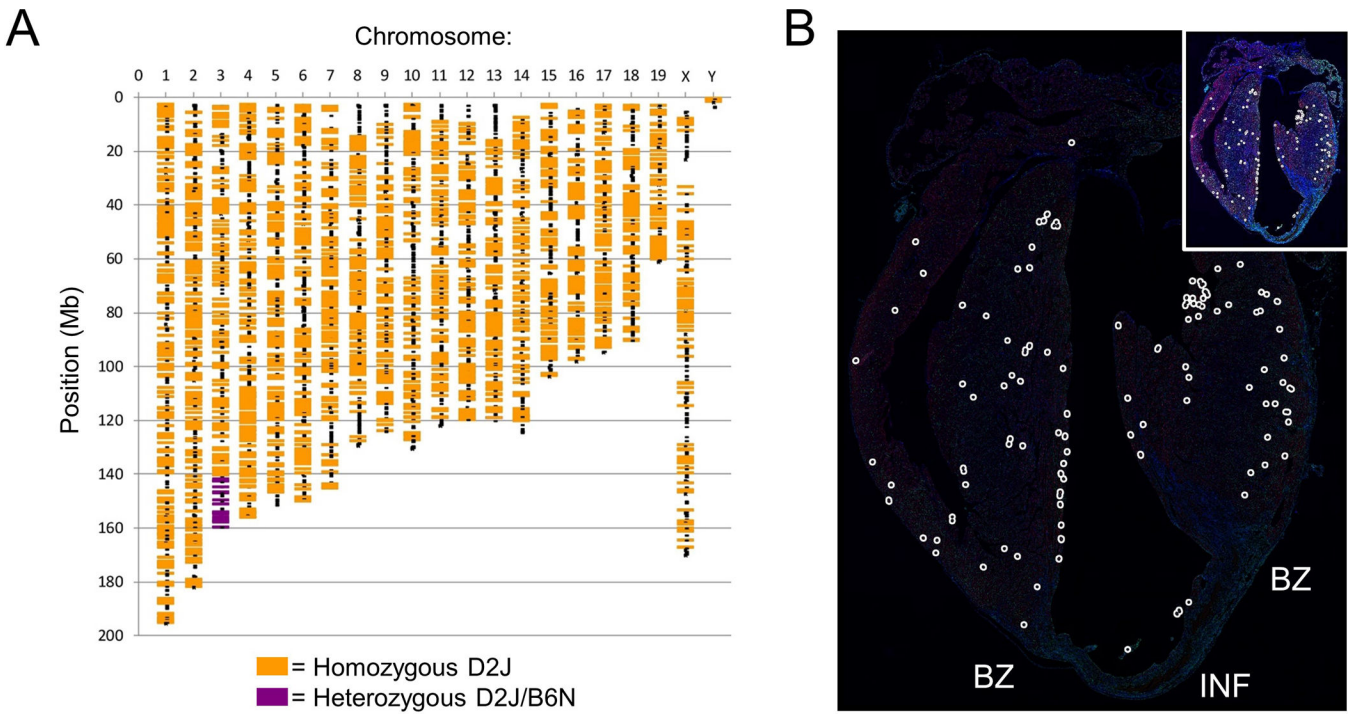

Figure 3.

Congenic mice heterozygous for the distal arm of chromosome 3 have high levels of cardiomyocyte S-phase activity post-injury. (A) SNP distribution map of the congenic mice; orange indicates homozygous D2J SNPs while purple indicates heterozygous D2J/B6N SNPs. (B) Representative example of a heart from a congenic mouse subjected to 14 days BrdU infusion immediately following permanent coronary artery ligation; a high level of cardiomyocyte S-phase activity is apparent in the remote myocardium (indicated by the white rings). Inset shows the same image with the brightness adjusted to facilitate visualization of the infarct anatomy at low magnification.

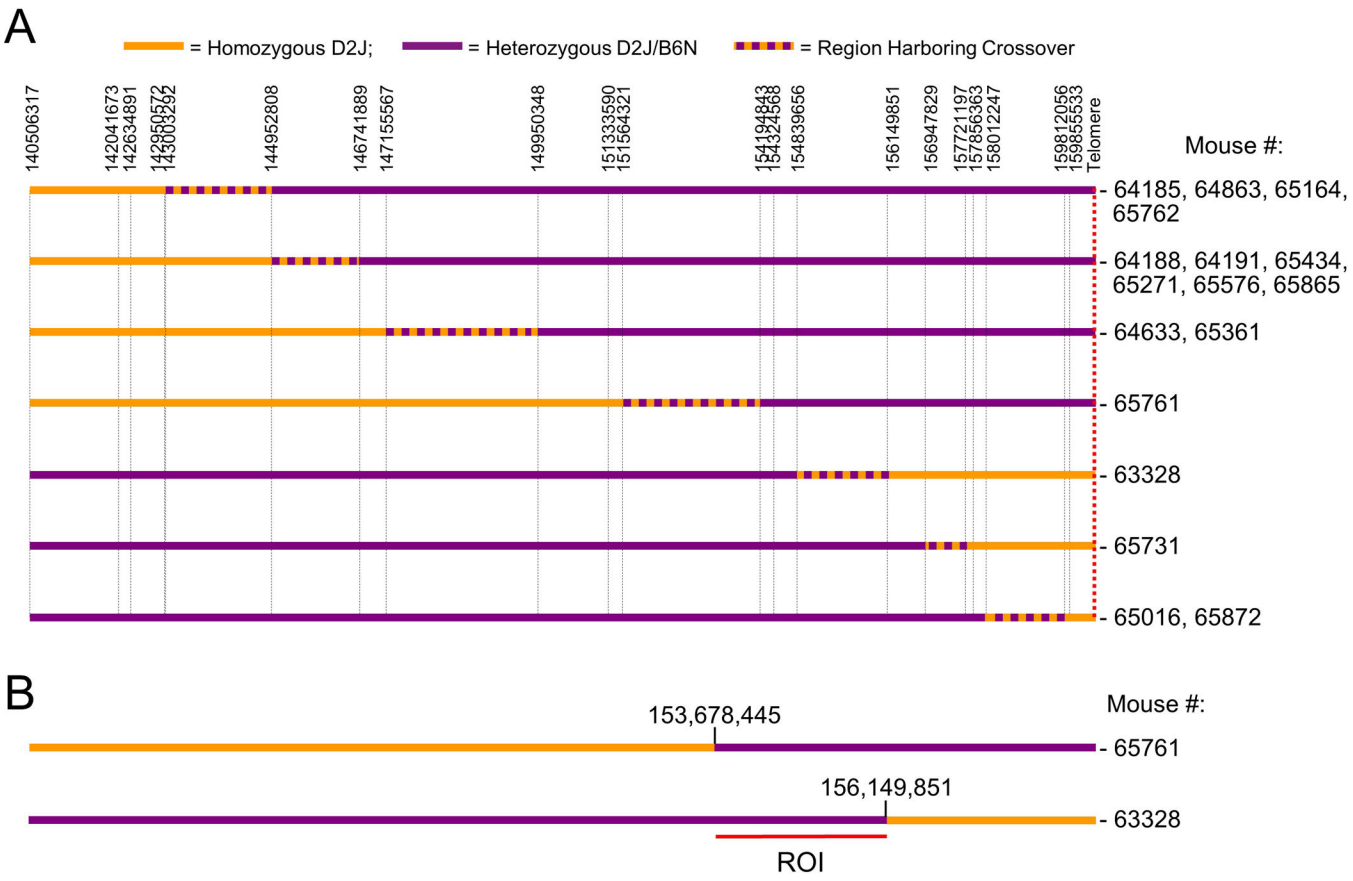

Figure 4.

Fine-scale mapping of a B6N allele which gives rise to high levels of cardiomyocyte S-phase activity following infarction. (A) SNP distribution on the distal arm of Chromosome 3 in [(D2J × B6N)-F1 × D2J] backcross mice with high rates of cardiomyocyte S-phase activity post-injury. Orange lines indicate chromosomal regions which are homozygous D2J, purple lines indicate chromosomal regions which are heterozygous D2J/B6N, and orange/purple dashes indicate chromosomal regions harboring a crossover event. (B) Proximal (in mouse #65761) and distal (in mouse #63328) boundary of the ROI as determined by WES analysis.

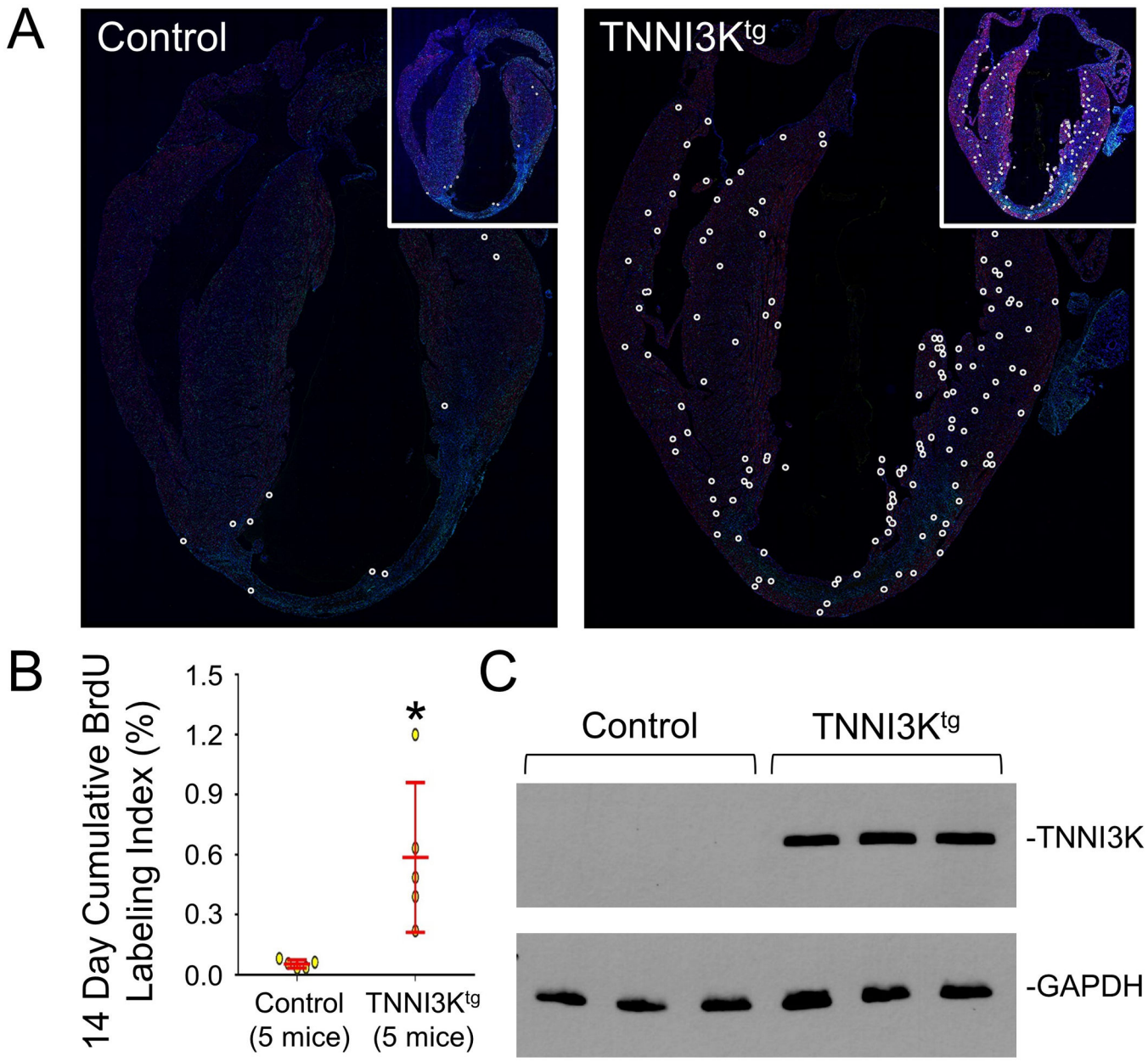

Figure 5.

Expression of human TNNI3K increases the level of cardiomyocyte S-phase activity in D2J mice following myocardial infarction. (A) Comparison of representative hearts from a control mouse and a TNNI3K^{tg} transgenic mouse which were subjected to 14 days BrdU infusion immediately following permanent coronary artery ligation (white rings indicate the position of S-phase cardiomyocyte nuclei). Insets show the same images with the brightness adjusted to facilitate visualization of the infarct anatomy at low magnification. (B) Cardiomyocyte S-phase labeling index in the remote myocardium after 14 days BrdU infusion in Control and TNNI3K^{tg} mice. Yellow markers indicate the labeling index for individual mice, while the wider horizontal red lines indicate the mean labeling index for a given genotype and the vertical red lines indicate the SEM; the asterisk indicates $p < 0.01$ vs.

Control mice by non-paired *t*-test. (C) Western blot demonstrating relative level of human TNNI3K protein expression in the TNNI3K^{tg} hearts.

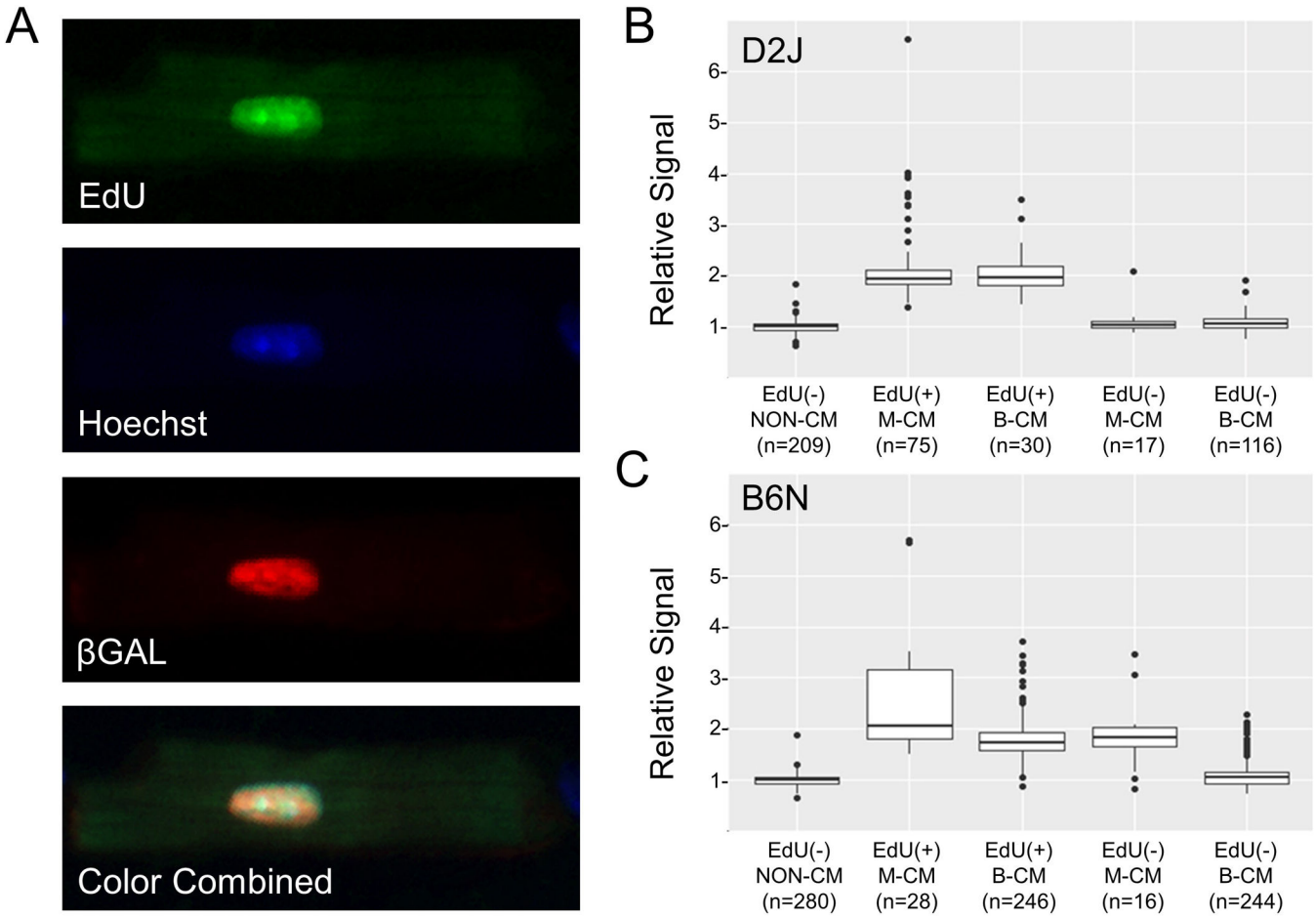

Figure 6.

Cardiomyocyte S-phase activity culminates in the formation of polyploid nuclei in the presence or absence of TNNI3K. (A) Example of an S-phase positive nucleus used to quantitate DNA content. The top panel shows EdU incorporation (green signal), the second panel shows Hoechst 33342 staining of DNA (blue signal), the third panel shows βGAL immune reactivity (red secondary antibody) and the bottom panel shows a color combined image. (B) Quantitation of nuclear DNA content in D2J mice at 14 days post-injury (EdU(−), EdU negative; EdU(+), EdU positive; NON-CM, non-cardiomyocyte; M-CM, mononucleated cardiomyocyte; B-CM, binucleated cardiomyocyte). The box extends from the 25th to 75th percentile (endpoints of the interquartile range (IQR)) with a line drawn at the median (50th percentile). The upper whisker is the maximum value of the data that is within 1.5 times the IQR over the 75th percentile. The lower whisker is the minimum value of the data that is within 1.5 times the IQR under the 25th percentile.. Points beyond that are shown as individual dots. Data was compiled from 6 mice, and “n” indicates the total number of nuclei for each cell type. (C) Quantitation of nuclear DNA content in B6N mice at 14 days post-injury. Labels and graph specifics are the same as for Panel B. Data was compiled from 4 mice, and “n” indicates the total number of nuclei for each cell type.